

AE-SiGMA ANALYSIS IN SPLIT-TENSILE TEST OF FIBER-REINFORCED CONCRETE (FRC) AT MESO-SCALE (*)

Mielke R.I.A.J Mondoringin

Sam Ratulangi University, Post Graduate Program
Civil Engineering Study Program, Manado, Indonesia
email: emilmondoringin03@yahoo.com

Masayasu Ohtsu

Kumamoto University, Graduate School of Science and Technology (GSST),
Dept. of Civil and Environmental Engineering, Japan.
email : ohtsu@gpo.kumamoto-u.ac.jp

ABSTRACT

Crack control plays a crucial role in the performance life of concrete structures. It presents a serious threat to the performance of concrete structures. Micro-cracking will appear when the strength of concrete is approached. Each of micro-cracks occurred inside concrete will produce a transient elastic wave which could be used to detect and localize cracks as well as to analyze kinematically the fracture mechanisms in concrete.

In this scientific paper, the SiGMA analysis is applied to the split-tensile tests of FRC to study the relation between the generation of macro-scale tensile crack and accumulation of meso-scale cracks as well as to know the role of the applied fiber on the cracking process of concrete.

Results showed that the relation between macro-scale tensile failure and nucleation of AE sources in meso-scale is clarified in Split-tensile test. At the macro-scale, tensile-type cracks are only observed, while all kinds of tensile, mixed-mode and shear cracks are identified at the meso-scale. During propagation of tensile cracks at the macro-scale, other types of AE sources of mixed-mode and shear cracks were actively identified.

Thus, nucleation of the fracture process zone is confirmed around the final failure surface. Mechanisms of macro-scale tensile failure process in concrete are clarified as the crack accumulation process at meso-scale determined by the SiGMA analysis. There exists a clear relation between macro-scale tensile failure process and nucleation of AE-sources in the meso-scale in the split-tensile test for the tensile strength of concrete.

KEYWORDS: AE-SiGMA, fracture, Split-tensile-test, tensile-cracks, FRC, AE hits, AE events

Note: () This paper had been presented in the International Conference on EFCM-held in Manado-Indonesia on 13 – 14 November 2014*

I. INTRODUCTION

Cracks present a serious threat to the performance of concrete structures and for this reason, methods allowing early detection and localization of cracks have been the subject of intensive investigations in the last few decades.

In this respect crack control plays a crucial role in the performance life of concrete structures. As a result, a variety of analytical, numerical and experimental investigations now exist. Concrete exhibits a particular behaviour namely micro-cracking when the strength of the material is

approached (Bazant, 1993; Labuz, and Biolzi, 1998).

Each of micro-crack occurred inside concrete produce a transient elastic wave. The non-destructive techniques could be used to monitor and also make predictions of crack occurred in concrete structure elements. Of the many non-destructive techniques available, acoustic emission (AE) technique is found to be the one of the most widely used to monitor, analyse and clarify the development processes of this micro-crack (Ohtsu and Ohtsuka 1998 ; Ohtsu *et al* 1998). In this respect, AE can play a significant role in the monitoring, predicting and clarifying the failure processes in civil engineering concrete structures since they are able to identify hidden defects leading to structural failures long before a collapse occurs and also in a real-time manner. Other merits of AE techniques are non-intrusive and monitor the whole volume in the area of interest (Ohtsu *et al* 1998). Since plain concrete always fail due to propagation of tensile cracks, the fracture mechanisms and tensile failure process of concrete need to be explored.

Fracture mechanisms in engineering materials can be kinematically identified by applying the moment tensor analysis of AE signal-based method (Ohtsu *et al* 1998, Akita *et al* 1998). Today, the moment tensor analysis of AE waveforms has been developed and is now available for identifying crack kinematics of a location, a crack-type and a crack orientation in concrete. The procedure has been implemented as the **SiGMA** (**S**implified **G**reen's functions for **M**oment tensor **A**nalysis) analysis (Ohtsu *et al* 1998, Akita *et al* 1998). It is demonstrated that mechanisms of cracking can be visually and quantitatively studied at the meso-scale in concrete. Since the tensile strength of concrete is normally evaluated by the split-tensile test, mechanisms of macro-scale tensile failure in concrete have been studied as the cracking process at the meso-scale as determined by the SiGMA analysis (Ohtsu *et al* 1998, Timoshenko and Goodier 1970).

Evolution of the fracture process zone under the combination of tensile and compressive stresses is discussed. Further we have clarified a

theoretical basis on the agreement of the tensile strengths of normal concrete in the split-tensile test and the direct tensile test, by applying the SiGMA analysis (Ohtsu and Ohtsuka 1998; Ohtsu *et al* 1998); Timoshenko and Goodier (1970). The failure process zone is created in a cross-section under constant tensile stress in the both tests. Thus, similar nucleation processes of the failure process zone could reasonably lead to comparable tensile strengths in the split-tensile test and the direct tensile. Recently, it is reported that the tensile strength of fiber-reinforced concrete is not straightforward to be estimated in the split-tensile test (Danneman *et al*, 2011; Mondoringin *et al*, 2011). In this respect, fracture mechanisms of fiber-reinforced concrete (FRC) in the split-tensile test are to be clarified at the meso-scale.

In this paper, the tensile failure process and the relation between the generation of macro-scale tensile cracks as well as the accumulation of meso-scale cracks of fiber reinforced concrete (FRC) concrete specimens are studied and then results are compared with those of mortar and normal concrete specimens using AE-SiGMA analysis. Thus, the role of applied fibers on the cracking process of concrete are successfully confirmed.

I. MATERIALS AND TEST PROCEDURE

1.1 Materials

In this experiment, concrete specimens were made into four types namely mortar, normal concrete, steel fiber-reinforced concrete (SFRC) and poly-vinyl-alcohol fiber reinforced concrete (PVAFRC). The specimens were compacted by external vibration. They were kept protected after casting to avoid evaporation, after 24 hours they were de-moulded and stored in room temperature until testing age was achieved. For all the mixtures, the maximum coarse aggregate size was 20 mm. By employing the ordinary Portland cement, the cut-fiber of 30 mm length was added by 0.1 % of SFRC and PVAFRC. For the split-tensile test, disc specimens of dimensions 150 mm diameter and 100 mm thickness were made. Mechanical properties of hardened concrete at 28-days are summerized in Table 2. Since the

volume ratio of fibers are just 0.1 %, the increase in the tensile strength of FRC are a little compared to that of normal concrete.

Table 1 Mechanical Properties of Hardened Concrete

Concrete	Compressive strength: σ_c (MPa)	Tensile strength: σ_t (MPa)	$\frac{\sigma_c}{\sigma}$ (%)
Mortar	29.1	2.19	9.5
Normal	23.9	2.3	9.6
SFRC	25.2	2.49	9.9
PVAFRC	23.8	2.64	11.1

2.2 Test Procedure

In order to identify and clarify the tensile failure process in concrete by AE-SiGMA, split tensile test were carried out to cylindrical specimens. AE signal were detected by employing AE Win SAMOS (PAC). Eight AE sensors of 150 kHz resonance (R151- AST) were attached to the specimen. The frequency range was 10 kHz to 2 MHz and total amplification was 60 dB gain (40 dB gain in a pre-amplifier and 20 dB in a main amplifier). The experimental set up are shown in Fig. 1. Eight specimens with four types of concrete were prepared. Prior to test, the sensor array was determined by a simulation analysis as shown in Fig.2, where AE source are assumed at lattice points with 5 mm grid at five cross-section of C₁ to C₅ at 5 mm apart. Based on the results of the simulation analysis, eight AE sensors were arranged as shown in Fig.3. It was found that computational errors of source locations were the minimum within 1.6 mm in the case of the sensor array shown in Fig.3 and their coordinates are given at Table 3. Thus the locations of 8 sensors were determined and the velocity of P waves was set to be 4010 m/s and arrival times were estimated with 1 sec. sampling.

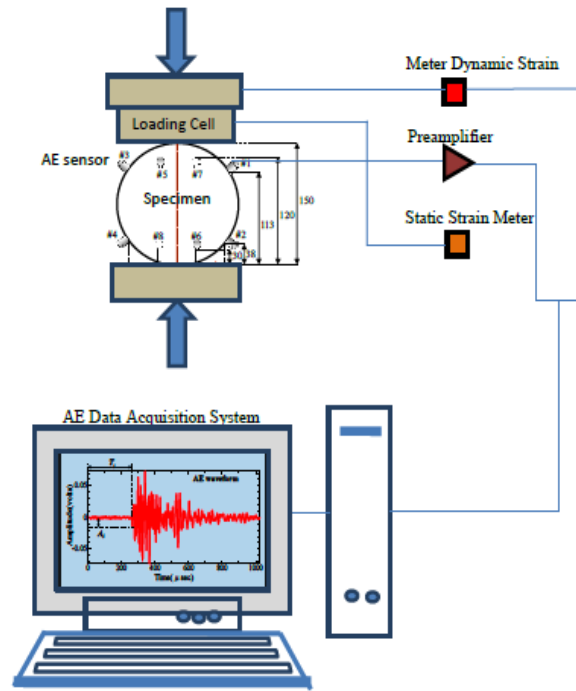


Fig. 1 Experimental Set up

Table 3 Optimal AE sensor array estimated for location analysis

Coordinates	X(cm)	Y(cm)	Z(cm)
Channel 1	6.5	2.5	11.3
Channel 2	6.5	7.5	3.8
Channel 3	6.5	7.5	11.3
Channel 4	6.5	2.5	3.8
Channel 5	4.0	0.0	1.2
Channel 6	4.0	0.0	3.0
Channel 7	4.0	10.0	12.0
Channel 8	4.0	10.0	3.0

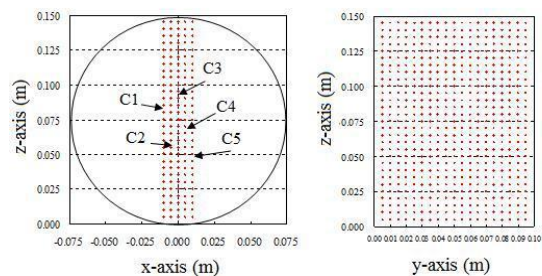


Fig. 2 Source location assumed in a simulation Analysis

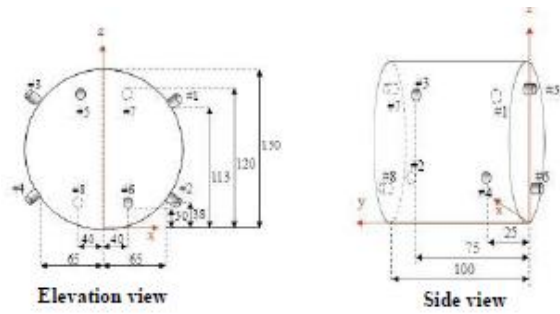
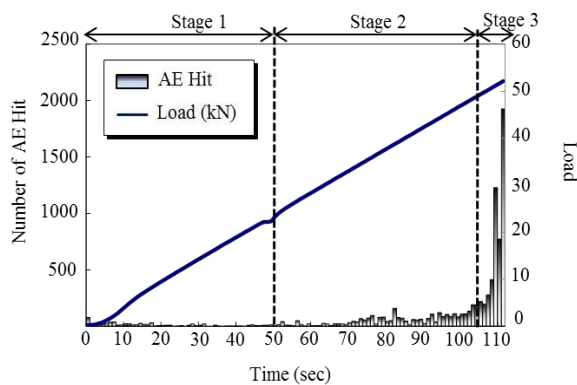


Fig.3 AE sensor array and cylindrical specimen, (unit in mm)

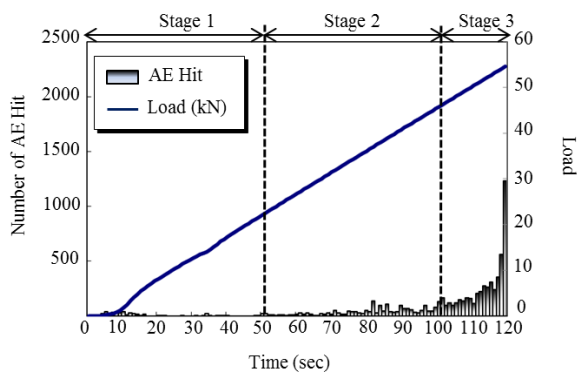
III. RESULTS AND DISCUSSION

3.1. Mortar and normal concrete specimen

The correlation of load and AE hits of mortar and normal concrete specimens are illustrated in figure 4.



(a) Mortar



(b) Normal Concrete

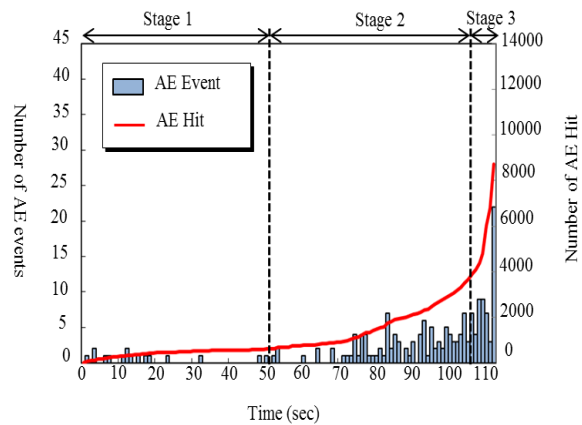
Fig. 4 The correlation between load and AE hits in mortar and normal concrete specimen

It can be seen from the figure 4.(a) for Mortar specimen that before 22 kN of applied load, there

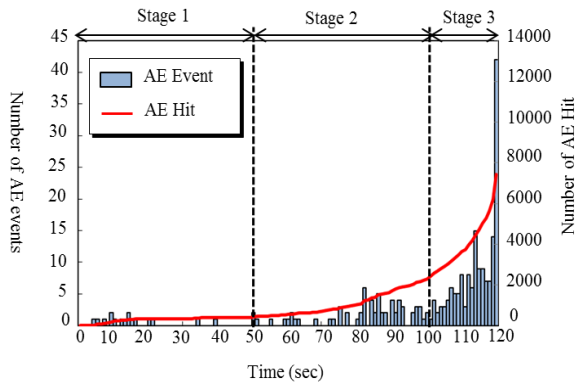
are only few or no significant AE hits are detected. Thus, almost no detectable crack occur. This is marked as the Stage 1 (0-50 seconds of time duration). In between 22 kN to 43 kN of applied load, the AE hits increase. This is marked as Stage 2. In this stage, it is observed that the micro-cracks start to randomly appear in the mortar specimen. Afterwards, once the applied load reaches its peak, a significantly larger amounts of AE hits increase abruptly within ten seconds, this is marked as the Stage 3 or final stage.

A relation between load and AE activity in normal concrete is shown in Fig. 4(b), AE hits, which imply the number of AE waves counted by all AE sensors, are actively observed at only the final stage. The stage corresponds to nucleation of the fracture process zone and crack at the macro-scale on one end to the whole cross section. As observed in Fig. 4(b), a few AE hits are observed until 25 kN of applied load. Then, in between 25 kN to 50 kN of applied load, AE hits increased gradually. Eventually, they reach their peak at 52 kN. Consequently, the illustrated as Stage 1, Stage 2, and Stage 3. AE waves of which the first motions were successfully detected at all 8 channels were analyzed to locate AE sources and then the SiGMA analysis was performed. These are named as AE events.

The number of AE hits represents AE activity, while AE events imply the numbers of AE sources analysed by SiGMA. A correlation between cumulative AE hits and AE events is given in Fig 5.



(a) Mortar

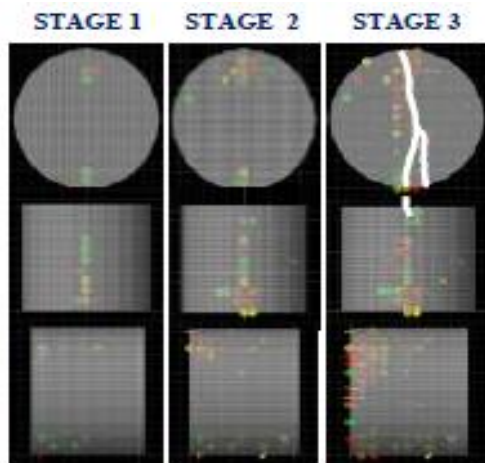


(a) Normal Concrete

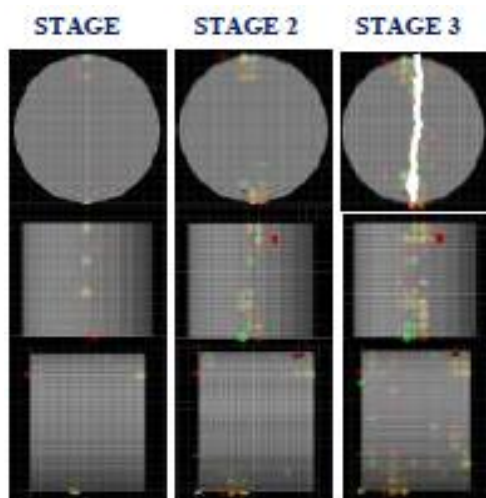
Fig. 5 Correlation of cumulative AE hits and AE events in (a) Mortar and (b).Normal Concrete specimen.

As shown in Fig.6, at Stage 1, AE sources are observed only near the loading plates in diametrical section (at Stage 1), where 15 AE-events of total 164 AE-events are identified. The dominant cracking modes are tensile and mixed-mode of 13 AE-events and shear mode of 2 AE-events. On Stage 2, cracks started at the contact of the loading plate and the specimen propagate into the center of specimen. After that, at Stage 3, a macro-crack is quickly formed and propagated to the center of the specimen, where the tensile stress reaches its maximum value as causing the specimen to be split apart as shown by white line in the specimen. In this time period, the shear mode increases dominantly compared to Stage 1 with 46 AE events. This indicates that the tensile, mixed - mode, and shear mode increase according to the rate of loading but the more dominant at Stage 3 is shear mode, which also implied that the tensile stress reaches it maximum value at Stage 3 and the crack opening becomes evident. Test results reveal that beyond the maximum tensile stress, the onset of crack nucleation starts and cracks propagate in parallel with the increase of shear mode. It also confirms that tensile cracks are dominant at the beginning of the cracking process of mortar specimen and then after the maximum tensile stress being reached, the shear cracks turn to become dominant over tensile cracks.

In order to investigate the fracture process of mortar, ratio of tensile, mixed-mode and shear cracks are compared in Fig 7.

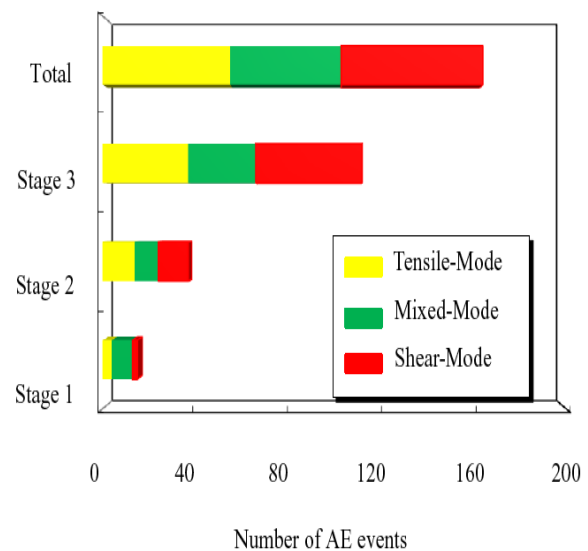


(a) Mortar

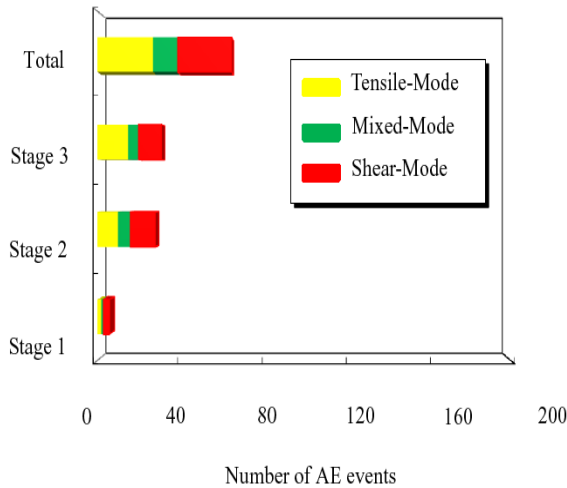


(b) Normal Concrete

Fig.6 Results of SiGMA analysis in Split-tensile test of mortar and normal specimen



(a).Mortar



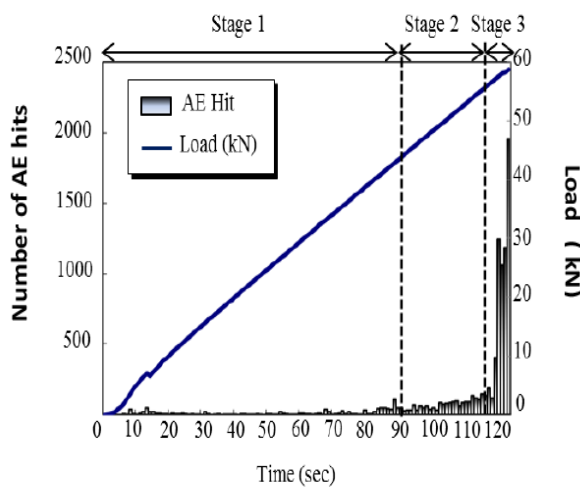
(b). Normal Concrete

Fig. 7 Crack modes analysed by SiGMA in mortar and normal specimen

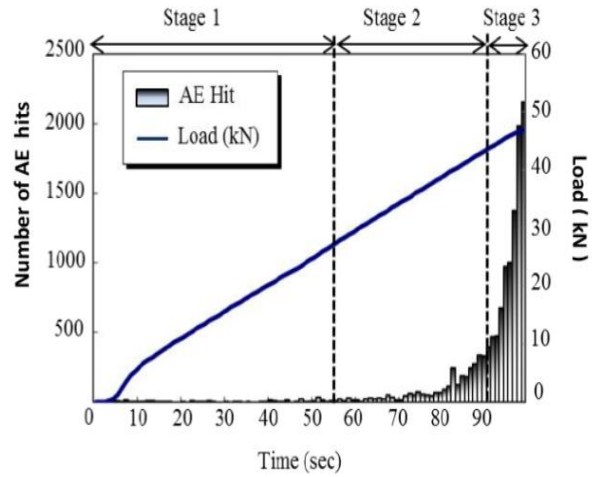
It is found that the number of analysed events gradually increases from Stage 1 to Stage 3. Concerning the ratios, the number of tensile cracks is dominant at Stage 1 and Stage 2, but at Stage 3, shear cracks increase abruptly and become dominant over tensile and mixed-mode cracks. Referring to the mixed-mode cracks as tensile cracks, it is realized that a half of cracks nucleated are tensile cracks at the meso-scale.

3.2. SFRC and PVAFRC Specimen

The relation between load and AE hits is illustrated in Fig.8,



(a)SFRC Specimen



(b) PVAFRC Specimen

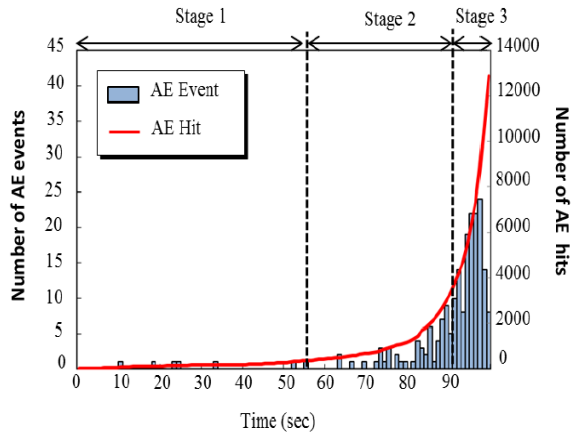
Fig. 8 The correlation between load and AE hits in SFRC and PVAFRC Specimen

AE activity under loading of SFRC again is classified into three stages as shown in figure 8(a). It is clearly observed that AE activity at Stage 3 is even higher than that of normal concrete. This suggests that more cracks are generated at the final stage. Before reaching around 42 kN of applied load at Stage 1, few AE hits are observed and thus cracks at the meso-scale are prevented by the reinforcing effect of fibers. In between 42 kN to 56 kN of applied load at Stage 2, AE hits are steadily observed. The fact might be associated with crack growth, which is somehow restricted by fibers. At Stage 3, AE hits are acceleratedly generated.

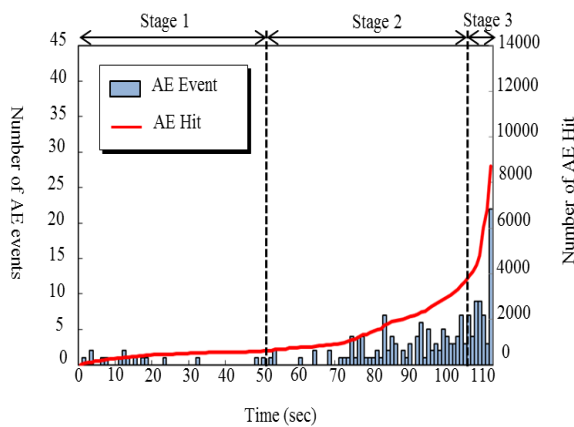
The mechanism of failure process of PVAFRC specimen are similar to SFRC specimen. The correlation of load and AE hits are illustrated in Fig.8(b). It can be seen that before 28 kN of applied load (0 to 56 seconds of time domain), there no significant AE-event were detected. This is marked as Stage 1. In between 28 kN to 42 kN of applied load, there is significant increasing of AE-hit which reached its peak at 98 seconds of its time domain. This might be associated with crack growth, that somehow restrained by fibers. And then afterwards, the AE-hits decreased gradually until 102 seconds.

The relation between accumulated number of AE hits and AE events in SFRC are shown in Fig. 9(a). Generating trend of AE events is similar to that of AE hits. So, it is understood that quite actively AE sources are observed at

only Stage 3. These AE sources possibly result from pulling-out of fibers, extension of tensile cracks and fretting of cracked surfaces. A correlation between cumulative AE hits and AE events in PVAFRC specimens are given in Fig 9.(b).



(a) SFRC Specimen



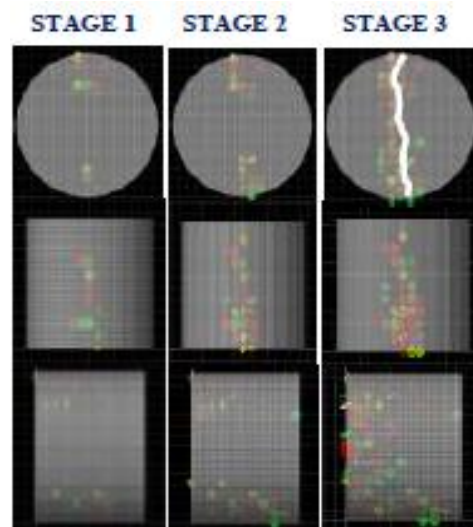
(b) PVAFRC

Fig. 9 Correlation of cumulative AE hits and AE events in SFRC and PVAFRC specimens

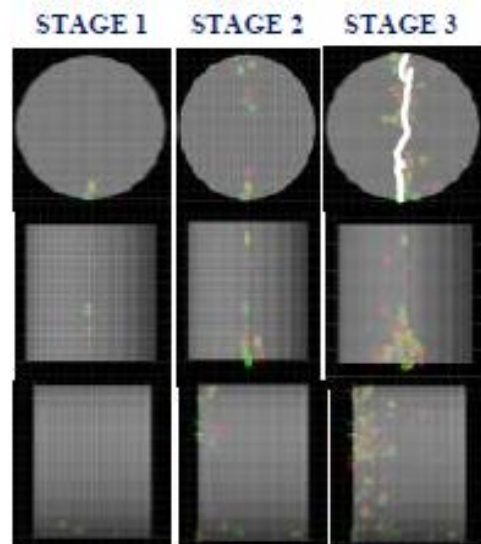
Results of AE-SiGMA analysis in SFRC and PVAFRC Specimens as shown in figure 10. There are 71 AE events in total were detected at this specimen. In Stage 1, there are only 5 tensile mode and 4 mixed-mode crack occurred. At Stage 2, the shear mode detected are increased abruptly namely 70 in total while the tensile mode increased moderately with 42 AE events and mixed-mode only increased 24 AE events. Similar to the steel fiber reinforced concrete, in this specimen, crack nucleation onset start at Stage 2, where micro-cracks start to develop by initially accompanied with a number of

increasing in AE events. When the strength of specimen material is reached, a macro-cracks is formed and at the moment, the dramatic increasing of AE event is detected, from 3 AE events in total at Stage 1 to 17 AE events in total at the Stage 2 (there is an increasing of 14 AE events).

Thereafter, as the loading continue, the cracks propagate widely into the center of the specimen while fibers bridging (90 to 95 seconds of time domain) that could be observed are gradually being pulled out from specimen and then fretting crack-surfaces created.



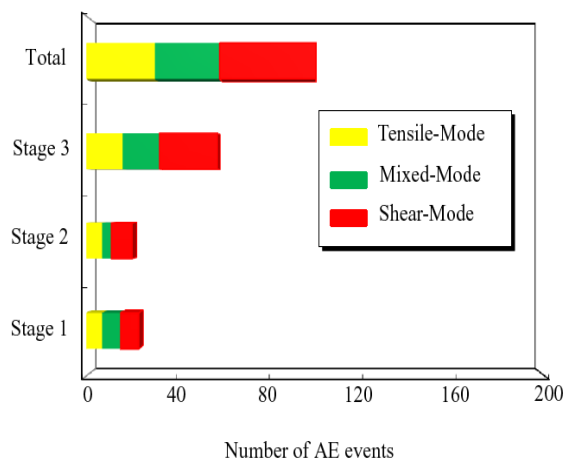
(a) SFRC Specimen



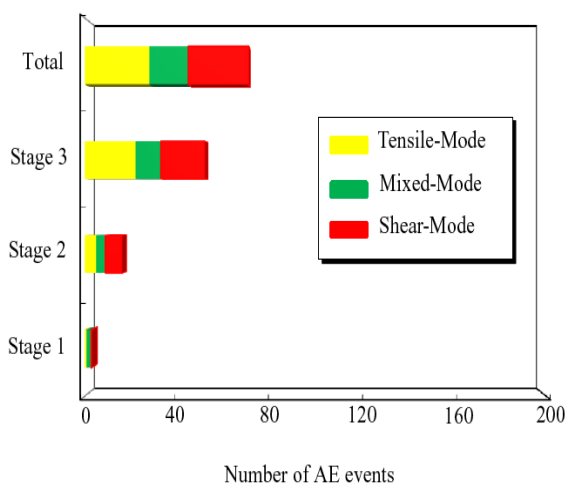
(b) PVA FRC Specimen

Fig.10 Results of SiGMA analysis in Split-tensile test of SFRC and PVAFRC specimen

The ratios of the tensile, mixed-mode and shear cracks of SFRC specimen are compared in Fig. 11.



(a) SFRC Specimen



(c) PVAFRC Specimen

Fig. 11 Crack modes analysed by SiGMA in SFRC and PVAFRC Specimens specimen

It is found that the number of analysed events at Stage 1 is similar to that of Stage 2, where the number of tensile cracks and mixed-mode is comparable to that of shear cracks. In comparison with Fig 11, the dominant increase of AE events is emphasized. Based on discussion before-mentioned, the number of the mixed-mode cracks is taken into account as other than tensile cracks. It is realized that the number of

AE sources other than tensile cracks including shear cracks is definitely dominant at Stage 3, suggesting nucleation of pulling-out fibers and fretting crack-surfaces created. Thus, under development of the fracture process zone in fiber-reinforced concrete, meso-scale cracks other than tensile cracks are actively generated in the split-tensile test. According to the study by Denneman et al.[8],two peaks of the loading curve are discussed, and they conclude that the 1st peak load should be used to estimate the tensile strength of fiber-reinforced concrete. Because the 1st peak might be observed following Stage 2, this strength could correspond to the strength of concrete constrained by fibers.

Results of cracks modes of SFRC Specimens and PVAFRC Specimens as shown in Fig. 11, revealed that the ratio of tensile cracks to mixed-mode and shear cracks are small in Stage 1, then at Stage 2, the ratio of tensile cracks plus mixed-mode-cracks as other than tensile cracks to shear cracks is comparable, but in Stage 3, shear cracks plus mixed-mode cracks suggesting nucleation of pulling out fibers and fretting crack surface created.

Based on the discussion, it is found some similarities of failure mechanisms among four types of concrete. Further this could be divides into two groups. The Group 1 is mortar and normal concrete specimens and the second one is SFRC and PVAFRC specimens. In the Group 1, it shown that after reached the peak loading, specimen being split apart, while in the second group, the specimen being bridging or restrained by fibers.

Regarding the failure mechanisms, the results of AE-SiGMA analysis are considered similar, as that start at the contact between the specimen and loading plate, and in the diametrical section they propagate to the center of the specimen. After the maximum tensile stress being reached, the specimen is split apart. Nevertheless, between Group 1 and Group 2, there is difference in Stage 3.

In Group 2, (both SFRC and PVAFRC), AE sources other than tensile cracks including shear cracks are definitely dominant over tensile cracks at Stage 3, suggesting that nucleation of pulling-

out fibers and fretting cracks surfaces created. Thus, under development of the fracture process zone in fiber-reinforced concrete, meso-scale cracks other than tensile cracks are actively generated in the split-tensile test.

I. CONCLUSION

The SiGMA analysis is applied to the Split-Tensile test of concrete cylinders.

- (1) A relation between macro-scale tensile failure and nucleation of AE sources in the meso-scale is clarified in the Split-Tensile test for the tensile strength of concrete.
- (2) At the macro-scale, tensile-type cracks are only observed, while all kinds of tensile, mixed-mode and shear cracks are identified at the meso-scale.
- (3) During propagation of tensile cracks at the macro-scale, other types of AE sources of mixed-mode and shear cracks were actively identified. Thus, nucleation of the fracture process zone is confirmed around the final failure surface.
- (4) Mechanisms of macro-scale tensile failure process in concrete are clarified as the crack accumulation process at meso-scale determined by the SiGMA analysis.
- (5) There exists a clear relation between macro-scale tensile failure process and nucleation of AE- sources in the meso-scale in the Split-Tensile test for the tensile strength of concrete.
- (6) This is a reason why the tensile strengths estimated by the Split-Tensile test are comparable to those by the direct-tensile test, although stress distributions are quite different.

ACKNOWLEDGEMENTS

The research conducted was supported by Kumamoto University Global COE (Center of Excellence) Program: Global Initiative Center for Pulsed Power Engineering. In order to perform experiments and analyses, the assistance of technical associate, Dr. Yuichi Tomoda was valuable. The authors wish to deeply thank all the supports.

REFERENCES

1. Bazant, Z.P (1993), ‘*Scaling Laws in Mechanics of Failure*’, J. Eng. Mech. ASCE.
2. Labuz, J.F, Biolzi, L.(1998), ‘*Characteristic Strength of Quasi-Brittle Materials*’, Int. J. Solids Struct., 35,31-32.:4191-4204.
3. Ohtsu, M, and Ohtsuka, M.(1998), ‘*Damage Evolution by Acoustic Emission in the Fracture Process Zone of Concrete*’, Proc. JSCE , 599-V40:177-184.
4. Ohtsu, M., Okamoto, T. and Yuyama, S. (1998), ‘*Moment Tensor Analysis of AE for Cracking Mechanisms in Concrete*’ , ACI Structural Journal, **95**(2): pp. 87-95.
5. Akita, H., Koide, H. and Tomon, M.,(1998), ‘*Uniaxial Tensile-Test of Un-notched Specimens under Correcting Flexure, Fracture Mechanics of Concrete Structures*’, Aedificatio Publishers, Freiburg, **1**: pp. 367-377.
6. Shah, K.R, Labuz, J. F.(1995), ‘*Damage Mechanisms in Stressed Rock from Acoustic Emission*’, J. Geophys. Res.,100,8.:15527-15539.
7. Timoshenko, S.P., and Goodier, J. N.,(1970), *Theory of Elasticity*, McGraw-Hill Book Company, New York.
8. Danneman, E, Kearsley, E.P, and Visser, A.T (2011), ‘*Splitting Tensile-Test for Fiber Reinforced Concrete*’, Material and Structure 44: 1441-1449. DOI 10.1617/s11527-011-9709-x.
9. Mondoringin, M., Nozaki, S., Ohtsu, M.,(2011), ‘*AE-SiGMA Analysis in Brazilian Test of Concrete*’ , Concrete Research Letters, ISSR Journal, Vol. 2 (**3**), pp. 267-270.